

Constraining the low-energy cosmic ray flux in the central molecular zone from MeV nuclear deexcitation line observations

Bing Liu^{1, 2, 3} and Ruizhi Yang^{1, 2, 3, *}

¹*Deep Space Exploration Laboratory, Hefei 230088, China*

²*CAS Key Laboratory for Research in Galaxies and Cosmology,
Department of Astronomy, School of Physical Sciences,*

University of Science and Technology of China, Hefei, Anhui 230026, China

³*School of Astronomy and Space Science, University of Science and Technology of China, Hefei, Anhui 230026, China*

Low-energy cosmic rays (LECRs) dominate the ionization in dense regions of molecular clouds in which other ionizers such as UV or X-ray photons are effectively shielded. Thus it was argued that the high ionization rate at the central molecular zone (CMZ) of our Galaxy is mainly caused by LECRs. However, the required LECR flux is orders of magnitude higher than the extrapolation of GeV cosmic ray (CR) flux derived from GeV γ -ray observations. In this paper, we considered two types of additional LECR components and found that only very soft anomalous CR components can explain such a high ionization rate. This LECR component will inevitably produce MeV nuclear deexcitation lines due to their inelastic scattering with the ambient gas. We calculated the MeV line emission and discussed the detectability of next-generation MeV instruments. We found that future MeV observations can be used to pin down the origin of the high ionization rate in the CMZ.

I. INTRODUCTION

Cosmic rays (CRs) are one of the most important components of the interstellar medium. Those with energy below 1 GeV per nucleon are usually referred to as low-energy CRs (LECRs). LECRs dominate the ionization and heating of dense molecular clouds, where the star forms, and also play an important role in the astrochemistry process [see,e.g., 1–3]. However, the measurement of LECRs is difficult, especially for LECRs with energy smaller than the production threshold of neutral pions (of about 280 MeV). LECRs suffer strong ionization loss and propagate slower in the standard propagation model [4]. Thus the density of LECRs in principle can be significantly different in different sites in our Galaxy.

In addition to indirect measurements such as the molecular ionization rate and Fe K α line emission [see,e.g., 5–7], γ -ray line emission from nuclear deexcitation is regarded as a unique tool for the probe of LECR nuclei, which can provide more abundant information on both accelerated particles and interacting medium [see,e.g., 8, 9]. Besides preresearch of MeV line emission around individual CR accelerators [see,e.g., 10–12], there were also several works done for the estimation of LECR-associated MeV line emission from the Galactic center (GC) [e.g., 13–15]. However, these estimations covered a much larger region around GC, and more specific structures can be analyzed and discussed regarding an ideal angular resolution ($\lesssim 2^\circ$ at MeV) that may be achieved by next-generation MeV γ -ray detectors.

In this regard, the central molecular zone (CMZ) in the center of our galaxy is of prime interest to such a study. Extending \sim 200 pc from the center (a GC distance of 8 kpc is applied in this paper), the CMZ holds around 10% of the Milky Way’s interstellar molecular mass [16]. Dense molecular clouds within the CMZ have

particle densities of around 10^4 cm^{-3} , fostering intense stellar activity and evolution, hosting numerous massive stars and supermassive clusters. It is marked by turbulent interstellar medium with strong magnetic fields, and energetic phenomena like supernova remnants and cataclysmic variables [17]. The CR ionization rates measured by astrochemistry methods are significantly higher in the CMZ than in other parts of our Galaxy[18]. This region offers insights into the complex dynamics of gas, magnetic fields, and stellar processes in the GC.

The CMZ has already been observed extensively in the entire electromagnetic radiation band. The high-energy CRs (HECRs, here referred as CRs with kinetic energy $> 1 \text{ GeV per nucleon}$) in the CMZ, which produce continuum gamma-ray emission via proton-proton inelastic collisions with the gases have been studied via various gamma-ray observations. Especially, the TeV γ -ray observations have revealed that CMZ harbor potential PeV CR accelerator [19], while in the GeV band, the CR density is even lower than in the vicinity [20, 21]. Thus a simple extrapolation seems to predict a lower LECR density in this region, and the corresponding ionization rate ($\zeta \sim 10^{-17} \text{s}^{-1}$) is several magnitudes lower than recent measurements ($\zeta \sim 2 \times 10^{-14} \text{s}^{-1}$,Oka *et al.* 22). Due to the very high gas density in the CMZ and effective shielding of UV and X-ray photons, the most probable source of ionization is the LECRs. The possible tension of the observations in different energy bands can be settled by assuming a new LECR component in the CMZ [14] or regarding that the high ionization rates are only valid for the surface of the molecular clouds [18]. In this paper, we calculated the MeV nuclear deexcitation line of LECRs in the CMZ. We found that the MeV line measurement with future MeV detectors can directly measure the CR density and distinguish the origin of the high ionization rate in CMZ, which would induce a significant impact in

understanding the star-forming processes in the GC.

This paper is organized as follows. In Sec.II, under the constraint of GeV-TeV gamma-ray observation, we describe the spectra distribution of CR combined with the assumed low-energy components in the CMZ. Next, in Sec.III, we calculate the corresponding ionization rate and 6.4-keV Fe K α line emission caused by CRs in the CMZ. Then in Sec.IV, we estimate the MeV nuclear deexcitation line emission generated by the interactions among CR nuclei and the gases in the CMZ. Finally, we discuss and summarize the above results in Sec.V.

II. SPECTRAL DISTRIBUTION AND COMPOSITIONS OF CRS IN CMZ

As mentioned above, the high ionization rate is in tension with the GeV γ -ray emission measured in the CMZ, which indicates another LECR component to provide the high ionization rate. In this work, we consider two scenarios for possible additional LECR nuclei accounting for the high ionization rate in the CMZ. One is the higher low-energy flux of the CRs predicted by the “concave” spectra in the previous theoretical nonlinear shock acceleration calculations [e.g., 23, 24]. Although such effects are insignificant in other nonlinear shock acceleration calculations [25], such concave spectral shape can also be formed in the situation when particles are reaccelerated by multiple shocks [e.g., 26]. The following calculations refer to such concave spectral shapes as scenario A. The other is possible anomalous CRs (ACRs), also dubbed the “carrot” component, accelerated from the F-, G-, and K-type stars or stellar winds from OB stars that reside in the CMZ (hereafter referred to as scenario B).

For scenario A, we assume the continuous injection of strong-shock accelerated or reaccelerated CRs has a piecewise power-law distribution to characterize the possible concavity of the injected spectra, as represented by Q_{in} [Eq.1]. Here, we set $E_b = 0.2 \text{ GeV}$, $\alpha_1 = 2.0$, and assume α_2 equal to α_1 or larger than α_1 , i.e., $\alpha_2 = 2.0, 2.5, 3.0, 3.5$, or 4.0 , to account for the possible concave structure. The CR proton density in the CMZ N_{lb} (in unit of $\text{GeV}^{-1}\text{cm}^{-3}$) is calculated using a simplified solution [Eq.2] of the leaky-box model, assuming the escape time of the protons, τ_{esc} , is $1.5 \times 10^7(E/1\text{GeV})^{-0.5} \text{ yr}$. Here, the energy loss time of the proton $\tau_{\text{loss}}(E, n)$ is approximated by $E/P(E, n)$, in which $P(E, n)$ represents the proton energy loss rate via ionization [1] and proton-proton inelastic collision [27] when propagating in gas medium with the average hydrogen density of the medium $n_{\text{H}} = 1 \text{ cm}^{-3}$. The fluxes of CR proton with $E < 1 \text{ MeV}$ are set to be zero and are not taken into account for the following calculations.

For scenario B, we assume the continuous injection of strong-shock accelerated CRs has a simple power-law distribution, i.e., set $\alpha_1 = \alpha_2 = 2.0$ for Q_{in} , and we calculate

corresponding proton density N_{lb} applying Eq.2. Then we add a local carrot component of density $N_c(E)$ represented by Eq.3, in which $\alpha = 4.0$ or 5.0 . Here, we vary factor f_c for different enhancements of low-energy CRs and set $E_{\text{cut}} = 1, 2, 4$, and 10 MeV , respectively.

$$Q_{\text{in}}(E) = \begin{cases} Q_0 \left[\frac{p(E)}{p(E_b)} \right]^{-\alpha_1}, & \text{if } E \geq E_b \\ Q_0 \left[\frac{p(E)}{p(E_b)} \right]^{-\alpha_2}, & \text{if } E < E_b \end{cases}. \quad (1)$$

$$N_{\text{lb}}(E) = Q_{\text{in}}(E) \left[\frac{1}{\tau_{\text{esc}}(E)} + \frac{1}{\tau_{\text{loss}}(E, n)} \right]^{-1} \quad (2)$$

$$N_c(E) = \begin{cases} f_c N_{\text{lb}}(E_b) \left[\frac{p(E)}{p(E_b)} \right]^{-\alpha}, & \text{if } E \geq E_{\text{cut}} \\ 0, & \text{if } E < E_{\text{cut}} \end{cases}. \quad (3)$$

For HECRs in the CMZ, according to recent GeV-TeV observation results [21], we fixed the proton energy density $w_p(80 \text{ GeV} \leq E_p \leq 5 \text{ TeV})$ to be 0.045 eV/cm^3 . Assuming a distance of 8 kpc for GC, the calculated differential fluxes of CR protons for scenarios A and B are exemplified in Fig.1.

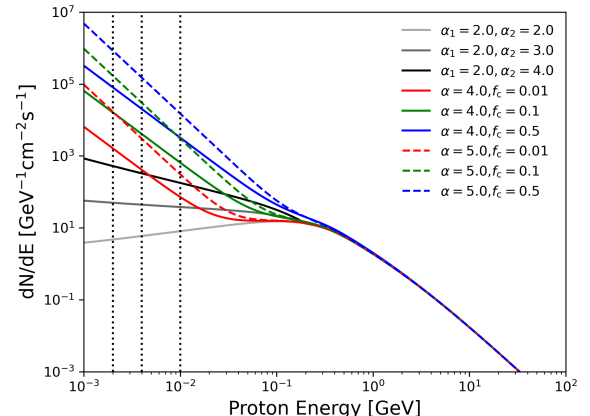


FIG. 1. Examples of the calculated differential flux of CR protons of scenario A with different α_1 and α_2 and scenario B with different α and f_c while setting $E_{\text{cut}} = 1 \text{ MeV}$. The vertical dotted lines indicate where other cutoff energies, i.e., $E_{\text{cut}} = 2, 4$, and 10 MeV , are set.

HECRs and LECRs are very likely associated with different sources; thus, the elemental composition of the CRs should vary with energy. In this work, for simplicity, we apply consistent compositions for both HECRs and LECRs. To estimate the indirect observable resulting from the interaction of CRs and the gases in the CMZ, we tested two different compositions for the CRs

TABLE I. The elemental compositions (number density ratio relative to H) applied for the calculations

	GCRS ^a	Local ^b	Solar ^c
H	1	1	1
He	6.90×10^{-2}	8.14×10^{-2}	8.41×10^{-2}
C	3.00×10^{-3}	1.67×10^{-3}	2.46×10^{-4}
N	1.37×10^{-4}	2.44×10^{-4}	7.24×10^{-5}
O	3.72×10^{-3}	1.57×10^{-3}	5.37×10^{-4}
Ne	2.82×10^{-4}	1.51×10^{-4}	1.12×10^{-4}
Mg	7.34×10^{-4}	2.26×10^{-4}	3.47×10^{-5}
Si	7.07×10^{-4}	1.90×10^{-4}	3.39×10^{-5}
S	9.24×10^{-5}	2.09×10^{-5}	1.45×10^{-5}
Ar	1.52×10^{-5}	4.55×10^{-6}	3.16×10^{-6}
Ca	4.20×10^{-5}	1.20×10^{-5}	2.04×10^{-6}
Fe	7.13×10^{-4}	1.15×10^{-4}	2.88×10^{-5}

^a The empirical GCR source composition [see 28, Table 1].

^b Voyager's measurement of local LECR abundance [see 29, Table 3].

^c The recommended present-day solar abundance [see 30, Table 6].

in the CMZ. One is the empirical GCR Source composition adopted from Table 1 of Meyer *et al.* 28 (hereafter referred to as GCRS composition), and the other is Voyager measurement of local LECR abundance listed in Table 3 of Cummings *et al.* 29 (hereafter referred to as the local composition). As for the gas content in the CMZ, we only apply solar abundances and solar abundances with twice the solar metallicity (hereafter referred to as double-solar or 2-solar composition), which is the same treatment done by Benhabiles-Mezhoud *et al.* [14]. The corresponding number density ratios relative to H of different compositions are listed in TableI.

Using a fixed total hydrogen mass, i.e., $M_H = 5 \times 10^7 M_\odot$, we then estimated the pion-decay gamma-ray emission fluxes in the CMZ applying the parametrized cross sections from Kafexhiu *et al.* [27]. As shown in Fig.1, the fluxes of protons with energy above the energy threshold (~ 280 MeV) of pion production process via proton-proton inelastic collision are basically the same for the tested parameters for both scenario A and scenario B. The resulting gamma-ray spectra show no obvious difference when varying the injected proton spectra parameters. When assuming different compositions of CRs and the gases, the enhancement factor calculated by Eq.(24) from Kafexhiu *et al.* [27] changes, and the gamma-ray fluxes change accordingly. As shown in Fig.2, the fluxes assuming a double-solar composition for gases in the CMZ are $\sim 20\%$ higher than that of solar abundance assumption; meanwhile, changing the CR composition from GCRs to local abundance measured by Voyager has minimal impact on the GeV gamma-ray fluxes. However, the predicted gamma-ray fluxes from the pion-decay process are consistent with the recent analysis results from Huang *et al.* [21] (data points in Fig.2). In short, the tested α_2 for scenario A and f_c for scenario B with the above elemental composition assumptions are consis-

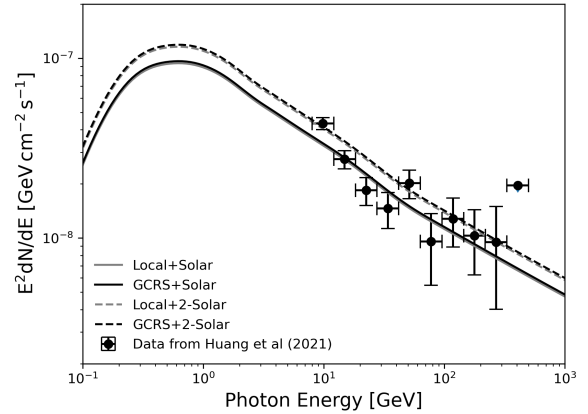


FIG. 2. The pion-decay emission calculated with different compositions for the CRs and gases in the CMZ when assuming a simple power-law injection ($\alpha_1 = \alpha_2 = 2.0$) of CR protons. The observation data is from Huang *et al.* [21].

tent with current GeV-TeV gamma-ray observations in the CMZ.

III. CONSTRAINT OF LECRS FROM MULTI-WAVELENGTH OBSERVATIONS TOWARDS CMZ

To constrain the possible LECR component in the CMZ, we then calculated the CR ionization rate of molecular hydrogen by applying formulas in Indriolo *et al.* [31] for the assumed CR spectra in Sec.2. Different assumptions of the elemental composition will influence the calculation results, for the ionization rate of molecular hydrogen, the results are ~ 1.5 times higher when using GCRS composition for CRs than the results obtained by applying local measurements from the Voyagers. For simplicity, here we only discuss the results obtained when assuming GCRS composition for CRs. As shown in Fig.3, without the additional LECRs, i.e., assuming a simple power-law injection ($\alpha_1 = \alpha_2 = 2.0$), the CR ionization for $E_p > 1$ MeV in the CMZ is about $1.3 \times 10^{-17} \text{ s}^{-1}$, which is three orders lower than the recent measurement ($\sim 2 \times 10^{-14} \text{ s}^{-1}$) made by Oka *et al.* [22]. For scenario A, the highest ionization rate is obtained while assuming $a_2 = 4.0$; however, the value $\sim 1.6 \times 10^{-16} \text{ s}^{-1}$ is still two orders lower than recent observation results. For scenario B, as shown in Fig.3, the value of E_{cut} has a significant influence on the calculated ionization rate, and the rate is two orders of magnitude lower when $E_{\text{cut}} = 10$ MeV comparing to that of $E_{\text{cut}} = 1$ MeV. Assuming $\alpha = 4.0$, the ionization rate reaches $\sim 2 \times 10^{-14} \text{ s}^{-1}$ when setting $f_c = 0.5$ and $E_{\text{cut}} = 1$ MeV, and the corresponding total energy density of the CR protons $W_p(E_p > 1 \text{ MeV})$ is 0.88 eV cm^{-3} . Meanwhile, if $\alpha = 5.0$, the lower energy

cutoff (E_{cut}) of the CR spectra should be higher than 2 MeV for $f_c = 0.2$ and higher than ~ 4 MeV for $f_c = 0.5$, of which the $W_p(E_p > 1 \text{ MeV}) < 1.3 \text{ eV cm}^{-3}$.

Furthermore, we estimated the total power to sustain such an additional carrot component in the CMZ (P_c) by applying Eq.4 adapted from Recchia *et al.* [32],

$$P_c = \int EN_c(E)V_{\text{cmz}}/\tau_{\text{loss}}(E, n_{\text{cmz}})dE \quad (4)$$

Here, $\tau_{\text{loss}}(E, n_{\text{cmz}}) \propto 1/n_{\text{H}} \propto V_{\text{cmz}}/M_{\text{H}}$. The required power for different setting of E_{cut} and f_c is shown in Fig.3. Under the constraints of the observed ionization rate, the total power to sustain such a carrot component in the CMZ is lower than $2 \times 10^{40} \text{ erg s}^{-1}$. This is a huge energy budget, but as mentioned above, such a low-energy ACR component is believed to be accelerated even in the low-mass F-type stars, considering the energy injection of all the stars in the CMZ, we cannot formally rule out such possibilities.

In addition, LECR nuclei are one of the causes of Fe K α line emissions in the GC. Thus, to estimate the contribution from the assumed carrot component, we calculated the corresponding 6.4-keV Fe K α line emission using cross sections given by Tatischeff *et al.* [7]. The total line fluxes are all lower than $10^{-4} \text{ ph cm}^{-2} \text{ s}^{-1}$ for the tested CR spectra even assuming double-solar abundance for the gases in the CMZ. The highest line flux is about $2 \times 10^{-5} \text{ ph cm}^{-2} \text{ s}^{-1}$, if the ionization rate caused by the additional LECR component $\leq 2 \times 10^{-14} \text{ s}^{-1}$. The 6.4-keV line flux caused by the possible additional LECR nuclei in the CMZ is below the observed total flux in the CMZ region [33]. Since the Fe K α line emission has multiple origins, such as hard X-ray photoionization and collisional ionization induced by CR electrons, our results are consistent with current X-ray observations toward the GC.

IV. MEV NUCLEAR DEEXCITATION LINE EMISSION IN THE CMZ

Under the constraint of ionization rate measurements, we calculated the possible nuclear deexcitation line emission from the interaction between CR nuclei and the gases towards the CMZ. Both narrow γ -ray lines from excited heavier elements of the ambient gas that collide with CR protons and α particles and broadened γ -ray lines from excited heavy nuclei of LECRs that interact with hydrogen and helium of the ambient gas are taken into account during the calculation. For the calculation process, except for the code TALYS which is the newest 1.96 version [34, 35], we applied the same procedure as described in Section 3.1 of Liu *et al.* [11], which followed the method developed by Ramaty *et al.* [8], Murphy *et al.* [9], Benhabiles-Mezhoud *et al.* [14]. Assuming GCRS and double-solar compositions for CR nuclei

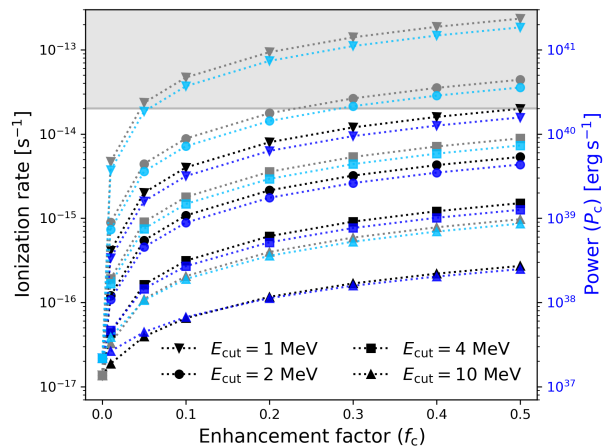


FIG. 3. The CR ionization rates of molecular hydrogen from the assumed local carrot component with GCRS composition and the power required to sustain the carrot component with different enhancement factors (f_c). The black ($\alpha=4.0$) data and the gray ($\alpha=5.0$) data are the ionization rates, meanwhile, the blue ($\alpha=4.0$) and light blue ($\alpha=5.0$) data represent the sustain power.

and gases in the CMZ respectively, the calculated differential nuclear deexcitation line emission flux for both scenario A and scenario B assuming different spectral parameters are exemplified in Fig.4. As shown in Fig.4, strong line emission can be found at energies such as 1.63, 4.44, and 6.13 MeV, which is mainly produced via the deexcitation of excited ^{20}Ne , ^{12}C , and ^{16}O . Using the above calculated MeV emission line spectra, we then estimated the 4.44- and 6.13-MeV line fluxes integrated for a linewidth of $\sim 100 \text{ keV}$. For scenario A, the highest fluxes, $\sim 1.44 \times 10^{-8} \text{ cm}^{-2} \text{ s}^{-1}$ for 4.44-MeV line and $\sim 4.53 \times 10^{-9} \text{ cm}^{-2} \text{ s}^{-1}$ for 6.13-MeV line, are obtained when assuming $\alpha_2 = 4.0$. Such fluxes are 5 times higher than a simple power-law assumption for the continuously injected CRs in the CMZ ($\alpha_1 = \alpha_2 = 2.0$). For scenario B, the line fluxes assuming different enhancements of additional carrot components and low-energy cutoffs are illustrated in Fig.5. Within the constraint of ionization rate ($\zeta \leq 2 \times 10^{-14} \text{ s}^{-1}$), assuming $\alpha = 4.0$, the highest fluxes of the 4.44-MeV line and the 6.13-MeV line, $\sim 1.6 \times 10^{-7} \text{ cm}^{-2} \text{ s}^{-1}$ and $\sim 3.5 \times 10^{-8} \text{ cm}^{-2} \text{ s}^{-1}$ respectively, are obtained when setting $E_{\text{cut}} \leq 4 \text{ MeV}$ and $f_c = 0.5$. Meanwhile, assuming $\alpha = 5.0$, the 4.44-MeV line and the 6.13 MeV line fluxes can reach $\sim 6.9 \times 10^{-7} \text{ cm}^{-2} \text{ s}^{-1}$ and $\sim 1.3 \times 10^{-7} \text{ cm}^{-2} \text{ s}^{-1}$ respectively when setting $E_{\text{cut}} = 4 \text{ MeV}$ and $f_c = 0.5$. Moreover, assuming a local composition for the CRs or solar abundance for the gases will yield lower fluxes for these line emissions, as also exemplified by the red and yellow data in Fig.5.

To discuss the possible detection of MeV line emission towards the CMZ, we must consider the influence of the

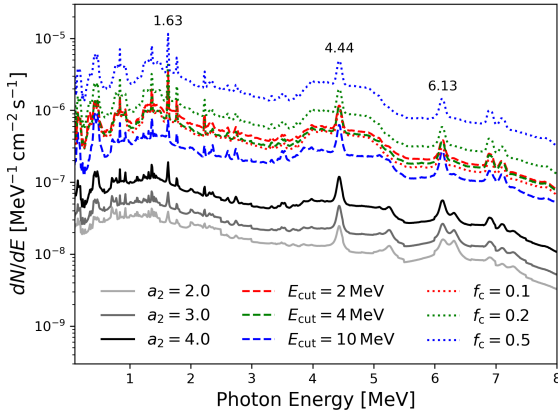


FIG. 4. Examples of the calculated MeV nuclear deexcitation line emission of scenario A and scenario B. Solid lines: scenario A with different α_2 while setting $\alpha_1 = 2.0$. Dashed lines: scenario B with different E_{cut} while setting $\alpha = 4.0$ and $f_c = 0.5$. Dotted lines: scenario B with different f_c while setting $\alpha = 5.0$ and $E_{\text{cut}} = 4.0$ MeV. The compositions of CR nuclei and gases in the CMZ are assumed to be GCRS and 2-solar respectively.

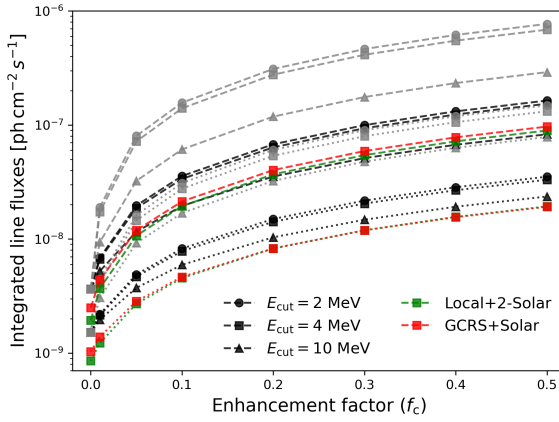


FIG. 5. The integrated fluxes of 4.44-MeV line (dashed lines) and 6.13-MeV line (dotted lines) from the CMZ under the assumption of different fractions of the carrot component f_c and E_{cut} . The black data show the results assuming $\alpha = 4.0$ and the grey data are obtained assuming $\alpha = 5.0$, assuming the compositions of CR nuclei and gases in the CMZ are assumed to be GCRS and 2-solar respectively. Setting $E_{\text{cut}} = 4$ MeV, the green data are obtained from the local (for the CRs)+2-solar (for the gases) assumption; meanwhile, the red data are obtained from the GCRS (for the CRs)+solar (for the gases) assumption.

MeV continuum background, which cannot be ignored in the GC region. Recently, using 16 years of INTEGRAL/SPI observation in the band 0.5-8.0 MeV, Siegert *et al.* [36] fitted the Galactic diffuse emission in a region of $\Delta l \times \Delta b = 95^\circ \times 95^\circ$ around the GC with energy-dependent IC scattering emission template acquired from

the GALPROP code [4], and found the spectrum of the diffuse gamma rays can be well described by a power law with an index of ~ -1.39 . Based on the energy-dependent spatial template and the spectrum of Galactic diffuse emission obtained by Siegert *et al.* [36], we extracted the diffuse gamma-ray emission spectrum within a radius of 2° around the GC, as the possible continuum MeV background when next-generation MeV telescopes with an angular resolution of $\sim 2^\circ$ observing the CMZ. As shown in Fig.6, the derived MeV diffuse gamma-ray flux within the 2° region around the GC is much higher than the MeV deexcitation line emission obtained from the assumed spectra of LECRs in the CMZ. Such a high background flux will make the MeV line research towards the CMZ very difficult. However, if the angular resolution of the next-generation MeV gamma-ray detectors could be improved to better than 2° at $\lesssim 10$ MeV, 1° for example, the chance of future detection of the deexcitation line emission from the CMZ will be significantly improved. As exemplified in Fig.6, the derived flux of the background MeV continuum for a region within a radius of 1° from GC is at the same level of the MeV deexcitation line emission obtained for extreme assumptions of LECRs in the CMZ, i.e., the high ionization rate is fully caused by the CR nuclei. Moreover, future detectors will resolve more MeV gamma-ray sources, thus, the background flux will be lower than our current estimation. Thus, we have a great opportunity to constrain these theories of the LECR distribution in the CMZ through the observation of MeV deexcitation line emission via next-generation MeV gamma-ray detectors.

V. SUMMARY

The extremely high ionization rate as high as $\sim 2 \times 10^{-14} \text{ s}^{-1}$ is observed in CMZ. The most probable ionizer in the dense region in CMZ is the LECRs. However, the GeV-TeV observations in CMZ reveal a similar HECR density in the CMZ as in the solar neighborhood, which implies an ionization rate 3 orders of magnitude smaller than observed. Thus, an additional LECR component is required. In this work, we consider two possible origins of the additional LECR component: one is from the concavity of the CR accelerated by strong shocks due to nonlinear effects or re-acceleration effects, and the other is the very soft carrot component accelerated from the F-, G-, and K-type stars or stellar winds from OB stars that reside in the CMZ. We found that only the latter can explain the extremely high ionization rate observed. If the CR ionization rate $\sim 2 \times 10^{-14} \text{ s}^{-1}$, we found that for $\alpha = 4.0$ and $E_{\text{cut}} = 1$ MeV, an enhancement factor [f_c in Eq.3] of 0.5 is required and if $\alpha = 5.0$, then $E_{\text{cut}} \geq 2$ MeV for $f_c = 0.2$ and $E_{\text{cut}} \geq 4$ MeV for $f_c = 0.5$. A total LECR energy budget of about $2 \times 10^{40} \text{ erg s}^{-1}$ is required in the above extreme case, which is huge but not impos-

DATA AVAILABILITY

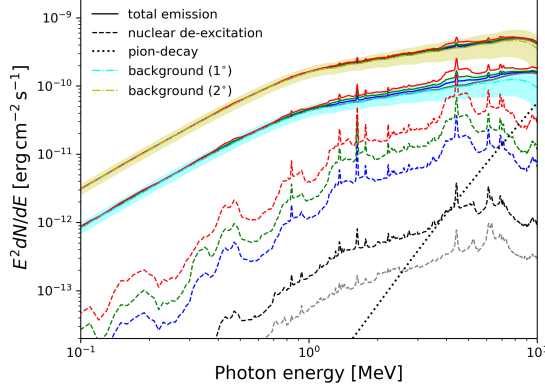


FIG. 6. Possible MeV gamma-ray emission from the CMZ with different scenarios of CR spectral distribution. The total emission (solid lines) includes emission from nuclear deexcitation (dashed lines) and pion-decay (dotted line) processes, as well as the continuum MeV background within different radii around the GC (dashed-dotted lines) derived by INTEGRAL/SPI data [36]. The shaded areas represent possible diffuse background emission with 1σ uncertainty. Red lines: $\alpha = 5.0$, $f_c = 0.5$, and $E_{\text{cut}} = 4 \text{ MeV}$ for scenario B. Green lines: $\alpha = 5.0$, $f_c = 0.2$, and $E_{\text{cut}} = 2 \text{ MeV}$ for scenario B. Blue lines: $\alpha = 4.0$, $f_c = 0.5$, and $E_{\text{cut}} = 1 \text{ MeV}$ for scenario B. Black lines: $\alpha_1 = 2.0$ and $\alpha_2 = 4.0$ for scenario A. Gray lines: $\alpha_1 = \alpha_2 = 2.0$ for scenario A. The compositions of CR nuclei and gases in the CMZ are assumed to be GCRS and 2-solar respectively.

sible.

Suppose additional LECR nuclei components mainly cause the high ionization rate in the CMZ. In that case, the predicted fluxes of the strong nuclear deexcitation lines can reach a level of $\sim 1 \times 10^{-6} \text{ ph cm}^{-2} \text{ s}^{-1}$ for 4.44-MeV line and $> 1 \times 10^{-7} \text{ ph cm}^{-2} \text{ s}^{-1}$ for 6.13-MeV line, which may be detected by the next-generation MeV instruments such as COSI [37], AMEGO [38] and MeGaT. However, the chemical composition of both LECRs and gases can considerably impact the MeV results. Due to the high continuum background in the GC region, both good spectral and angular resolution are required to detect these MeV deexcitation lines. In particular, the width of the nuclear deexcitation lines can be as high as several percent ($\sim 100 \text{ keV}$) mainly due to the kinematics [8]. Thus the angular resolutions play a more important role in detecting such kinds of MeV emissions. In this regard, the next-generation MeV instruments with an angular resolution similar to or better than 1° are very promising to test such a hypothesis and solve the mysterious origin of the high ionization rate in the CMZ. Such in situ measurement of the LECR spectrum would also help to understand the possible dynamic effects of the LECR component in the CMZ as well as the possible impact on the star-formation process in this complex region.

To calculate emissivities of the deexcitation γ -ray line lines, we used the code TALYS (version 1.96, Koning *et al.* 34), which could be downloaded from https://tendl.web.psi.ch/tendl_2019/talys.html. For a better match with the experiment data, we modified the deformation files of ^{14}N , ^{20}Ne , and ^{28}Si using the results of Benhabiles-Mezhoud *et al.* [39]. We also used the production cross sections of the specific lines listed in the compilation of Murphy *et al.* [9].

ACKNOWLEDGEMENTS

Bing Liu acknowledges the support from the NSFC under grant 12103049. Rui-zhi Yang is supported by the NSFC under grants 12041305, and 12393854.

* yangrz@ustc.edu.cn

- [1] M. Padovani, D. Galli, and A. E. Glassgold, Cosmic-ray ionization of molecular clouds, *A&A* **501**, 619 (2009), arXiv:0904.4149 [astro-ph.SR].
- [2] P. P. Papadopoulos, A Cosmic-ray-dominated Interstellar Medium in Ultra Luminous Infrared Galaxies: New Initial Conditions for Star Formation, *ApJ* **720**, 226 (2010), arXiv:1009.1134 [astro-ph.CO].
- [3] S. Gabici, Low-energy cosmic rays: regulators of the dense interstellar medium, *A&ARv* **30**, 4 (2022), arXiv:2203.14620 [astro-ph.HE].
- [4] A. E. Vladimirov, S. W. Digel, G. Jóhannesson, P. F. Michelson, I. V. Moskalenko, P. L. Nolan, E. Orlando, T. A. Porter, and A. W. Strong, GALPROP WebRun: An internet-based service for calculating galactic cosmic ray propagation and associated photon emissions, *Computer Physics Communications* **182**, 1156 (2011), arXiv:1008.3642 [astro-ph.HE].
- [5] N. Indriolo, G. A. Blake, M. Goto, T. Usuda, T. Oka, T. R. Geballe, B. D. Fields, and B. J. McCall, Investigating the Cosmic-ray Ionization Rate Near the Supernova Remnant IC 443 through H^+ 3 Observations, *ApJ* **724**, 1357 (2010), arXiv:1010.3252 [astro-ph.HE].
- [6] N. Indriolo, D. A. Neufeld, M. Gerin, P. Schilke, A. O. Benz, B. Winkel, K. M. Menten, E. T. Chambers, J. H. Black, S. Bruderer, E. Falgarone, B. Godard, J. R. Goicoechea, H. Gupta, D. C. Lis, V. Ossenkopf, C. M. Persson, P. Sonnenrecker, F. F. S. van der Tak, E. F. van Dishoeck, M. G. Wolfire, and F. Wyrowski, Herschel Survey of Galactic OH^+ , H_2O^+ , and H_3O^+ : Probing the Molecular Hydrogen Fraction and Cosmic-Ray Ionization Rate, *ApJ* **800**, 40 (2015), arXiv:1412.1106 [astro-ph.GA].
- [7] V. Tatischeff, A. Decourchelle, and G. Maurin, Nonthermal X-rays from low-energy cosmic rays: application to the 6.4 keV line emission from the Arches cluster region, *A&A* **546**, A88 (2012), arXiv:1210.2108 [astro-ph.HE].

- [8] R. Ramaty, B. Kozlovsky, and R. E. Lingenfelter, Nuclear gamma-rays from energetic particle interactions., *ApJS* **40**, 487 (1979).
- [9] R. J. Murphy, B. Kozlovsky, J. Kiener, and G. H. Share, Nuclear Gamma-Ray De-Excitation Lines and Continuum from Accelerated-Particle Interactions in Solar Flares, *ApJS* **183**, 142 (2009).
- [10] A. Summa, D. Elsässer, and K. Mannheim, Nuclear de-excitation line spectrum of Cassiopeia A, *A&A* **533**, A13 (2011), arXiv:1107.4331 [astro-ph.HE].
- [11] B. Liu, R.-z. Yang, and F. Aharonian, Nuclear de-excitation lines as a probe of low-energy cosmic rays, *A&A* **646**, A149 (2021), arXiv:2101.03695 [astro-ph.HE].
- [12] B. Liu, R.-z. Yang, X.-y. He, and F. Aharonian, New estimation of the nuclear de-excitation line emission from the supernova remnant Cassiopeia A, *MNRAS* **524**, 5248 (2023), arXiv:2307.08967 [astro-ph.HE].
- [13] V. A. Dogiel, V. Tatischeff, K. S. Cheng, D. O. Chernyshov, C. M. Ko, and W. H. Ip, Nuclear interaction gamma-ray lines from the Galactic center region, *A&A* **508**, 1 (2009), arXiv:0909.2110 [astro-ph.HE].
- [14] H. Benhabiles-Mezhoud, J. Kiener, V. Tatischeff, and A. W. Strong, De-excitation Nuclear Gamma-Ray Line Emission from Low-energy Cosmic Rays in the Inner Galaxy, *ApJ* **763**, 98 (2013), arXiv:1212.1622 [astro-ph.HE].
- [15] A. de Angelis, V. Tatischeff, I. A. Grenier, J. McEnery, M. Mallamaci, M. Tavani, U. Oberlack, L. Hanlon, R. Walter, A. Argan, P. von Ballmoos, A. Bulgarelli, A. Bykov, M. Hernanz, G. Kanbach, I. Kuvvetli, M. Pearce, A. Zdziarski, J. Conrad, G. Ghisellini, A. Harding, J. Isern, M. Leising, F. Longo, G. Madejski, M. Martinez, M. N. Mazziotta, J. M. Paredes, M. Pohl, R. Rando, M. Razzano, A. Aboudan, M. Ackermann, A. Addazi, M. Ajello, C. Albertus, J. M. Álvarez, G. Ambrosi, S. Antón, L. A. Antonelli, A. Babic, B. Baibussinov, M. Balbo, L. Baldini, S. Balman, C. Bambi, U. Barres de Almeida, J. A. Barrio, R. Bartels, D. Bastieri, W. Bednarek, D. Bernard, E. Bernardini, T. Bernasconi, B. Bertucci, A. Biland, E. Bissaldi, M. Boettcher, V. Bonvicini, V. Bosch-Ramon, E. Bottacini, V. Bozhilov, T. Bretz, M. Branchesi, V. Brdar, T. Bringmann, A. Brogna, C. Budtz Jørgensen, G. Busetto, S. Buson, M. Busso, A. Caccianiga, S. Camera, R. Campana, P. Caraveo, M. Cardillo, P. Carlson, S. Celestin, M. Cermeño, A. Chen, C. C. Cheung, E. Churazov, S. Ciprini, A. Coc, S. Colafrancesco, A. Coleiro, W. Collmar, P. Coppi, R. Curado da Silva, S. Cutini, F. D’Ammando, B. de Lotto, D. de Martino, A. De Rosa, M. Del Santo, L. Delgado, R. Diehl, S. Dietrich, A. D. Dolgov, A. Domínguez, D. Domínis Prester, I. Donnarumma, D. Dorner, M. Doro, M. Dutra, D. Elsaesser, M. Fabrizio, A. Fernández-Barral, V. Fioretti, L. Foffano, V. Formato, N. Fornengo, L. Foschini, A. Franceschini, A. Franckowiak, S. Funk, F. Fuschino, D. Gaggero, G. Galanti, F. Gargano, D. Gasparini, R. Gehrz, P. Giannaria, N. Giglietto, P. Giommi, F. Giordano, M. Giroletti, G. Ghirlanda, N. Godinovic, C. Gouiffés, J. E. Grove, C. Hamadache, D. H. Hartmann, M. Hayashida, A. Hryczuk, P. Jean, T. Johnson, J. José, S. Kaufmann, B. Khelifi, J. Kiener, J. Knöldseder, M. Kole, J. Kopp, V. Kozhuharov, C. Labanti, S. Lalkovski, P. Laurent, O. Limousin, M. Linares, E. Lindfors, M. Lindner, J. Liu, S. Lombardi, F. Loparco, R. López-Coto, M. López Moya, B. Lott, P. Lubrano, D. Malyshev, N. Mankuzhiyil, K. Mannheim, M. J. Marchā, A. Marcianò, B. Marcote, M. Mariotti, M. Marisaldi, S. McBreen, S. Mereghetti, A. Merle, R. Mignani, G. Minervini, A. Moiseev, A. Morselli, F. Moura, K. Nakazawa, L. Nava, D. Nieto, M. Orienti, M. Orio, E. Orlando, P. Orleanski, S. Paiano, R. Paoletti, A. Papitto, M. Pasquato, B. Patricelli, M. Á. Pérez-García, M. Persic, G. Piano, A. Pichel, M. Pimenta, C. Pittori, T. Porter, J. Poutanen, E. Prandini, N. Prantzos, N. Produit, S. Profumo, F. S. Queiroz, S. Rainó, A. Raklev, M. Regis, I. Reichardt, Y. Rephaeli, J. Rico, W. Rodejohann, G. Rodriguez Fernandez, M. Roncadelli, L. Roso, A. Rovero, R. Ruffini, G. Sala, M. A. Sánchez-Conde, A. Santangelo, P. Saz Parkinson, T. Sbarrato, A. Shearer, R. Shellard, K. Short, T. Siegert, C. Siqueira, P. Spinelli, A. Stamerra, S. Starfield, A. Strong, I. Strümke, F. Tavecchio, R. Taverna, T. Terzić, D. J. Thompson, O. Tibolla, D. F. Torres, R. Turolla, A. Ulyanov, A. Ursi, A. Vacchi, J. van den Abeele, G. Vankova-Kirilovai, C. Venter, F. Verrecchia, P. Vincent, X. Wang, C. Weniger, X. Wu, G. Zaharijaš, L. Zampieri, S. Zane, S. Zimmer, A. Zoglauer, and E-Astrogam Collaboration, Science with e-ASTROGAM. A space mission for MeV-GeV gamma-ray astrophysics, *Journal of High Energy Astrophysics* **19**, 1 (2018), arXiv:1711.01265 [astro-ph.HE].
- [16] R. Genzel, D. Hollenbach, and C. H. Townes, The nucleus of our galaxy, *Reports on Progress in Physics* **57**, 417 (1994).
- [17] M. Morris and E. Serabyn, The galactic center environment, *Annual Review of Astronomy and Astrophysics* **34**, 645 (1996).
- [18] V. A. Dogiel, D. O. Chernyshov, A. M. Kiselev, M. Nobukawa, K. S. Cheng, C. Y. Hui, C. M. Ko, K. K. Nobukawa, and T. G. Tsuru, Spectrum of Relativistic and Subrelativistic Cosmic Rays in the 100 pc Central Region, *ApJ* **809**, 48 (2015), arXiv:1507.02440 [astro-ph.HE].
- [19] HESS Collaboration, A. Abramowski, F. Aharonian, F. A. Benkhali, A. G. Akhperjanian, E. O. Angüner, M. Backes, A. Balzer, Y. Becherini, J. B. Tjus, D. Berge, S. Bernhard, K. Bernlöhr, E. Birsin, R. Blackwell, M. Böttcher, C. Boisson, J. Bolmont, P. Bordas, J. Bregeon, F. Brun, P. Brun, M. Bryan, T. Bulik, J. Carr, S. Casanova, N. Chakraborty, R. Chalme-Calvet, R. C. G. Chaves, A. Chen, M. Chrétien, S. Colafrancesco, G. Cologna, J. Conrad, C. Couturier, Y. Cui, I. D. Davids, B. Degrange, C. Deil, P. Dewilt, A. Djannati-Ataï, W. Domainko, A. Donath, L. O. Drury, G. Dubus, K. Dutson, J. Dyks, M. Dyrda, T. Edwards, K. Egberts, P. Eger, J. P. Ernenwein, P. Espigat, C. Farnier, S. Fegan, F. Feinstein, M. V. Fernandes, D. Fernandez, A. Fiasson, G. Fontaine, A. Förster, M. Füßling, S. Gabici, M. Gajdus, Y. A. Gallant, T. Garrigoux, G. Giavitto, B. Giebels, J. F. Glicenstein, D. Gottschall, A. Goyal, M. H. Grondin, M. Grudzińska, D. Hadasch, S. Häffner, J. Hahn, J. Hawkes, G. Heinzelmann, G. Henri, G. Hermann, O. Hervet, A. Hillert, J. A. Hinton, W. Hofmann, P. Hofverberg, C. Hoischen, M. Höller, D. Horns, A. Ivascenko, A. Jacholkowska, M. Jamrozy, M. Janiak, F. Jankowsky, I. Jung-Richardt, M. A. Kastendieck, K. Katarzyński, U. Katz, D. Kerszberg, B. Khélifi, M. Kieffer, S. Klepser, D. Klochkov, W. Kluzniak, D. Kolitzus,

- N. Komin, K. Kosack, S. Krakau, F. Krayzel, P. P. Krüger, H. Laffon, G. Lamanna, J. Lau, J. Lefaucheur, V. Lefranc, A. Lemiére, M. Lemoine-Goumard, J. P. Lenain, T. Lohse, A. Lopatin, C. C. Lu, R. Lui, V. Marandon, A. Marcowith, C. Mariaud, R. Marx, G. Maurin, N. Maxted, M. Mayer, P. J. Meintjes, U. Menzler, M. Meyer, A. M. W. Mitchell, R. Moderski, M. Mohamed, K. Morå, E. Moulin, T. Murach, M. de Naurois, J. Niemiec, L. Oakes, H. Odaka, S. Öttl, S. Ohm, B. Opitz, M. Ostrowski, I. Oya, M. Panter, R. D. Parsons, M. P. Arribas, N. W. Pekeur, G. Pelletier, P. O. Petrucci, B. Peyaud, S. Pita, H. Poon, H. Prokoph, G. Pühlhofer, M. Punch, A. Quirrenbach, S. Raab, I. Reichardt, A. Reimer, O. Reimer, M. Renaud, R. de Los Reyes, F. Rieger, C. Romoli, S. Rosier-Lees, G. Rowell, B. Rudak, C. B. Rulten, V. Sahakian, D. Salek, D. A. Sanchez, A. Santangelo, M. Sasaki, R. Schlickeiser, F. Schüssler, A. Schulz, U. Schwanke, S. Schwemmer, A. S. Seyffert, R. Simoni, H. Sol, F. Spanier, G. Spengler, F. Spies, L. Stawarz, R. Steenkamp, C. Stegmann, F. Stinzing, K. Styrcz, I. Sushch, J. P. Tavernet, T. Tavernier, A. M. Taylor, R. Terrier, M. Tluczykont, C. Trichard, R. Tuffs, K. Valerius, J. van der Walt, C. van Eldik, B. van Soelen, G. Vasileiadis, J. Veh, C. Venter, A. Viana, P. Vincent, J. Vink, F. Voisin, H. J. Völk, T. Vuillaume, S. J. Wagner, P. Wagner, R. M. Wagner, M. Weidinger, Q. Weitzel, R. White, A. Wiercholska, P. Willmann, A. Wörlein, D. Wouters, R. Yang, V. Zabalza, D. Zaborov, M. Zacharias, A. A. Zdziarski, A. Zech, F. Zefi, and N. Źywucka, Acceleration of petaelectronvolt protons in the Galactic Centre, *Nature* **531**, 476 (2016), arXiv:1603.07730 [astro-ph.HE].
- [20] Yang, Rui-zhi, de Oña Wilhelmi, Emma, and Aharonian, Felix, Probing cosmic rays in nearby giant molecular clouds with the fermi large area telescope, *A&A* **566**, A142 (2014).
- [21] X. Huang, Q. Yuan, and Y.-Z. Fan, A GeV-TeV particle component and the barrier of cosmic-ray sea in the Central Molecular Zone, *Nature Communications* **12**, 6169 (2021), arXiv:2012.05524 [astro-ph.HE].
- [22] T. Oka, T. R. Geballe, M. Goto, T. Usuda, Benjamin, J. McCall, and N. Indriolo, The Central 300 pc of the Galaxy Probed by Infrared Spectra of H_3^+ and CO. I. Predominance of Warm and Diffuse Gas and High H₂ Ionization Rate, *ApJ* **883**, 54 (2019), arXiv:1910.04762 [astro-ph.HE].
- [23] E. Amato and P. Blasi, A general solution to non-linear particle acceleration at non-relativistic shock waves, *MNRAS* **364**, L76 (2005), arXiv:astro-ph/0509673 [astro-ph].
- [24] D. Caprioli, P. Blasi, and E. Amato, Non-linear diffusive acceleration of heavy nuclei in supernova remnant shocks, *Astroparticle Physics* **34**, 447 (2011), arXiv:1007.1925 [astro-ph.HE].
- [25] D. Caprioli, Cosmic-ray acceleration in supernova remnants: non-linear theory revised, *J. Cosmology Astropart. Phys.* **2012**, 038 (2012), arXiv:1206.1360 [astro-ph.HE].
- [26] T. Vieu, S. Gabici, and V. Tatischeff, Non-linear particle reacceleration by multiple shocks, *MNRAS* **510**, 2529 (2022), arXiv:2109.10639 [astro-ph.HE].
- [27] E. Kafexhiu, F. Aharonian, A. M. Taylor, and G. S. Vila, Parametrization of gamma-ray production cross sections for p p interactions in a broad proton energy range from the kinematic threshold to PeV energies, *Phys. Rev. D* **90**, 123014 (2014), arXiv:1406.7369 [astro-ph.HE].
- [28] J.-P. Meyer, L. O. Drury, and D. C. Ellison, A Cosmic-ray Composition Controlled by Volatility and a/q Ratio. SNR Shock Acceleration of gas and Dust, *Space Sci. Rev.* **86**, 179 (1998).
- [29] A. C. Cummings, E. C. Stone, B. C. Heikkila, N. Lal, W. R. Webber, G. Jóhannesson, I. V. Moskalenko, E. Orlando, and T. A. Porter, GALACTIC COSMIC RAYS IN THE LOCAL INTERSTELLAR MEDIUM: VOYAGER 1 observations AND MODEL RESULTS, *The Astrophysical Journal* **831**, 18 (2016).
- [30] K. Lodders, Solar System Abundances of the Elements, *Astrophysics and Space Science Proceedings* **16**, 379 (2010), arXiv:1010.2746 [astro-ph.SR].
- [31] N. Indriolo, B. D. Fields, and B. J. McCall, The Implications of a High Cosmic-Ray Ionization Rate in Diffuse Interstellar Clouds, *ApJ* **694**, 257 (2009), arXiv:0901.1143 [astro-ph.HE].
- [32] S. Recchia, V. H. M. Phan, S. Biswas, and S. Gabici, Can a cosmic ray carrot explain the ionization level in diffuse molecular clouds?, *MNRAS* **485**, 2276 (2019), arXiv:1901.04912 [astro-ph.HE].
- [33] H. Uchiyama, M. Nobukawa, T. G. Tsuru, and K. Koyama, K-Shell Line Distribution of Heavy Elements along the Galactic Plane Observed with Suzaku, *PASJ* **65**, 19 (2013), arXiv:1209.0067 [astro-ph.HE].
- [34] A. J. Koning, S. Hilaire, and M. C. Duijvestijn, TALYS-1.0, in *Proceedings of the International Conference on Nuclear Data for Science and Technology, April 22-27, 2007, Nice, France*, EDP Sciences, edited by O. Bersillon, F. Gunsing, E. Bauge, R. Jacqmin, and S. Leray (2008) pp. 211–214.
- [35] A. Koning, D. Rochman, and S. van der Marck, Extension of talys to 1 gev, *Nuclear Data Sheets* **118**, 187 (2014).
- [36] T. Siegert, J. Bertaud, F. Calore, P. D. Serpico, and C. Weinberger, Diffuse Galactic emission spectrum between 0.5 and 8.0 MeV, *A&A* **660**, A130 (2022), arXiv:2202.04574 [astro-ph.HE].
- [37] J. A. Tomsick, S. E. Boggs, A. Zoglauer, D. Hartmann, M. Ajello, E. Burns, C. Fryer, C. Karwin, C. Kierans, A. Lowell, J. Malzac, J. Roberts, P. Saint-Hilaire, A. Shih, T. Siegert, C. Sleator, T. Takahashi, F. Tavecchio, E. Wulf, J. Beechert, H. Gulick, A. Joens, H. Lazar, E. Neights, J. C. Martinez Oliveros, S. Matsumoto, T. Melia, H. Yoneda, M. Amman, D. Bal, P. von Ballmoos, H. Bates, M. Böttcher, A. Bulgarelli, E. Cavazzuti, H.-K. Chang, C. Chen, C.-Y. Chu, A. Ciabattoni, L. Costamante, L. Dreyer, V. Fioretto, F. Fenu, S. Gallego, G. Ghirlanda, E. Grove, C.-Y. Huang, P. Jean, N. Khatiya, J. Knöldlseder, M. Krause, M. Leising, T. R. Lewis, J. P. Lommler, L. Marcotulli, I. Martinez-Castellanos, S. Mittal, M. Negro, S. Al Nussirat, K. Nakazawa, U. Oberlack, D. Palmore, G. Panebianco, N. Parmiggiani, T. Parsotan, S. N. Pike, F. Rogers, H. Schutte, Y. Sheng, A. P. Smale, J. Smith, A. Trigg, T. Venter, Y. Watanabe, and H. Zhang, The Compton Spectrometer and Imager, *arXiv e-prints*, arXiv:2308.12362 (2023), arXiv:2308.12362 [astro-ph.HE].
- [38] J. McEnery, A. van der Horst, A. Dominguez, A. Moiseev, A. Marcowith, A. Harding, A. Lien, A. Giuliani,

- A. Inglis, S. Ansoldi, A. Stamerra, A. Manousakis, A. Strong, C. Bambi, B. Patricelli, M. Baring, J. A. Barrio, D. Bastieri, B. Fields, J. Beacom, V. Beckmann, W. Bednarek, B. Rani, S. Boggs, A. Bolotnikov, S. B. Cenko, J. Buckley, B. Grefenstette, M. Hui, C. Pittori, C. Prescod-Weinstein, C. Shrader, C. Gouiffes, C. Kierans, C. Wilson-Hodge, F. D'Ammando, D. Castro, D. Kocvessi, D. Gasparrini, D. Thompson, D. Williams, A. De Angelis, D. Bernard, S. Digel, D. Morcuende, E. Charles, E. Bissaldi, E. Hays, E. Ferrara, E. Bozzo, E. Grove, E. Wulf, E. Bottacini, E. Caroli, F. Kislat, F. Oikonomou, F. Giordano, F. Longo, C. Fryer, Y. Fukazawa, M. Georganopoulos, G. De Nolfo, G. Vianello, G. Kanbach, G. Younes, H. Blumer, D. Hartmann, M. Hernanz, H. Takahashi, H. Li, I. Agudo, I. Moskalenko, I. Stumke, I. Grenier, J. Smith, J. Rodi, J. Perkins, J. Gelfand, J. Holder, J. Knodlseder, J. Kopp, J.-P. Lenain, J.-M. Álvarez, J. Metcalfe, J. Krizmanic, J. B. Stephen, J. Hewitt, J. Mitchell, P. Harding, J. Tom-sick, J. Racusin, J. Finke, O. Kargaltsev, A. V. Klimenko, H. Krawczynski, K. Smith, H. Kubo, L. Di Venere, L. Marcotulli, J. Lommler, L. Parker, L. Baldini, L. Fofano, L. Zampieri, L. Tibaldo, M. Petropoulou, M. Ajello, M. Meyer, M. López, M. McConnell, M. Boettcher, M. Cardillo, M. Martinez, M. Kerr, M. N. Mazzotta, J. McEnery, M. Di Mauro, M. Wood, E. Meyer, M. Briggs, M. De Becker, M. Lovellette, M. Doro, M. A. Sanchez-Conde, M. Moss, T. Mizuno, M. Ribó, K. Nakazawa, N. K. Neilson, N. Auricchio, N. Omodei, U. Oberlack, M. Ohno, E. Orlando, N. Otte, P. Coppi, P. Bloser, H. Zhang, P. Laurent, M. Pohl, E. Prandini, P. Shawhan, R. Caputo, R. Campana, R. Rando, R. Woolf, R. Johnson, R. Mignani, R. Walter, R. Ojha, R. C. da Silva, S. Dietrich, S. Funk, S. Zane, S. Anton, S. Buson, S. Cutini, P. Saz Parkinson, R. Schirato, S. Griffin, S. Kaufmann, L. Stawarz, S. Ciprini, S. Del Sordo, S. Jones, S. Guiriec, H. Tajima, T. Cheung, L.-S. The, T. Venter, T. Porter, T. Linden, U. Barres, V. S. Paliya, V. Bozhilov, T. Vestrand, V. Tatischeff, W. Chen, X. Wang, Y. Tanaka, L. Uhm, B. Zhang, S. Zimmer, A. Zoglauer, and Z. Wadiasingh, All-sky Medium Energy Gamma-ray Observatory: Exploring the Extreme Multi-messenger Universe, in *Bulletin of the American Astronomical Society*, Vol. 51 (2019) p. 245, arXiv:1907.07558 [astro-ph.IM].
- [39] H. Benhabiles-Mezhoud, J. Kiener, J. P. Thibaud, V. Tatischeff, I. Deloncle, A. Coc, J. Duprat, C. Hamadache, A. Lefebvre-Schuh, J. C. Dalouzy, F. de Grancey, F. de Oliveira, F. Dayras, N. de Séville, M. G. Pellegriti, L. Lamia, and S. Ouichaoui, Measurements of nuclear γ -ray line emission in interactions of protons and α particles with N, O, Ne, and Si, Phys. Rev. C **83**, 024603 (2011), arXiv:1011.2561 [nucl-ex].